Electronic supplementary materials *Mendeleev Commun.*, 2026, **36**, 21–24

Coordination-driven self-assembly of pentacopper metallamacrocycles with *N*-(3-hydroxy-2-methyl-4-oxopyridin-1-yl)isonicotinamide units for antimycobacterial activity

Marina A. Katkova, Roman V. Rumyantcev, Galina S. Zabrodina, Irina G. Fomina, Olga B. Bekker, Grigory Yu. Zhigulin, Sergey Yu. Ketkov and Igor L. Eremenko

Table of Contents

General details

All reagents were obtained from commercial sources or synthesized as detailed in Table S1. The elemental analysis was performed using EuroVector CHNS-O Elemental Analyzer Euro EA 3000. IR spectra (IRS) were recorded on a Perkin Elmer Spectrum 65 spectrophotometer equipped with a Quest ATR Accessory (Specac) by the attenuated total reflectance (ATR) in the range of 400–4000 cm^{-1}.

*Synthesis of [(Cu_5(β-alaha$_4$)](CuL_2)(H_2O)$_{26}$ (**1**)*

[Cu_5(β-alaha$_4$)](CuL_2)(H_2O)$_{26}$ (**1**): β-alaninehydroxamic acid (0.104 g, 1 mmol) was dissolved in 20 mL of water and added to a stirred solution of $Cu(ac)_2 \cdot H_2O$ (0.299 g, 1.5 mmol) in 20 mL of water at room temperature. The reaction mixture immediately turns a deep blue-green colour. Then, a water solution of N-(3-Hydroxy-2-methyl-4-oxo-4H-pyridin-1-yl)-isonicotinamide (0.12 g, 0.5 mmol) was slowly added at controlled pH values above 8.5, and the mixture was stirred for two hours. After filtration the green solution was left to evaporate slowly at room temperature. X-Ray suitable green crystals were obtained after a few days. Yield 0,27 g (61 %), m.p. > 260 (decomposition). Anal. Calcd. for $C_{36}H_{94}Cu_6N_{14}O_{40}$ (1744.49): C, 24.79; H, 5.43; N, 11.24 %. Found: C, 24.85; H, 5.51; N, 11.18 %.

Single-crystal X-ray structure analysis

To analyze the obtained data (indexing, data integration, frame scaling and absorption correction), we used the CrysAlisPro software package.[S3] The structure was solved by dual method[S4] and refined on F^2_{hkl} using SHELXTL package.[S5] All non-hydrogen atoms were refined anisotropically. The hydrogen atoms in all water molecules in crystal **1** were located from difference Fourier maps and were refined with geometric restrictions (DFIX command) and restrictions on ADPs (U_{iso}(H) = 1.2U_{eq}(O)). All other hydrogen atoms were placed in calculated positions and were refined in the riding model [U_{iso}(H) = 1.5U_{eq}(C) for CH_3-group and U_{iso}(H) = 1.2U_{eq}(C) for other groups].

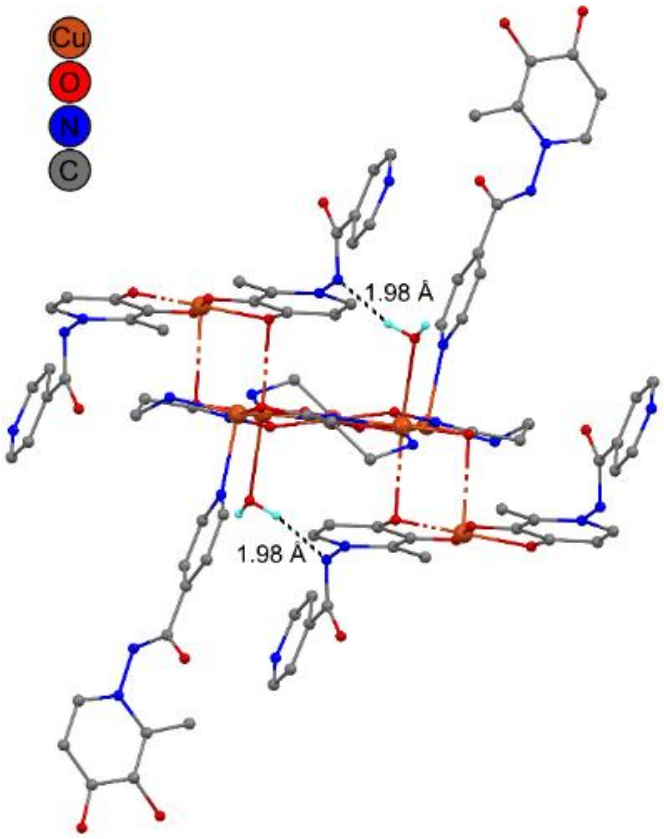

Figure S1. Fragment of the 3D structure of compound **1**, which shows the environment of the metallamacrocyclic cation. Hydrogen atoms are omitted.

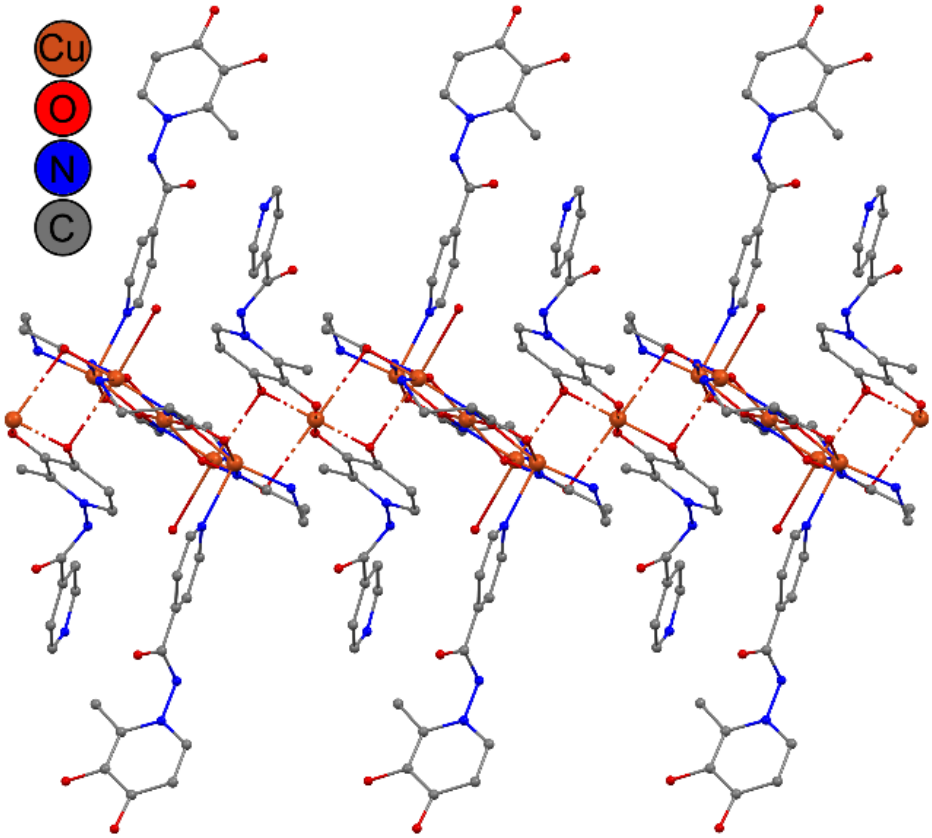

Figure S2. Fragment of an one-dimensional chain (-[Cu_5(β-alaha$_4$)]-[CuL_2]-)$_n$ in crystal **1**.

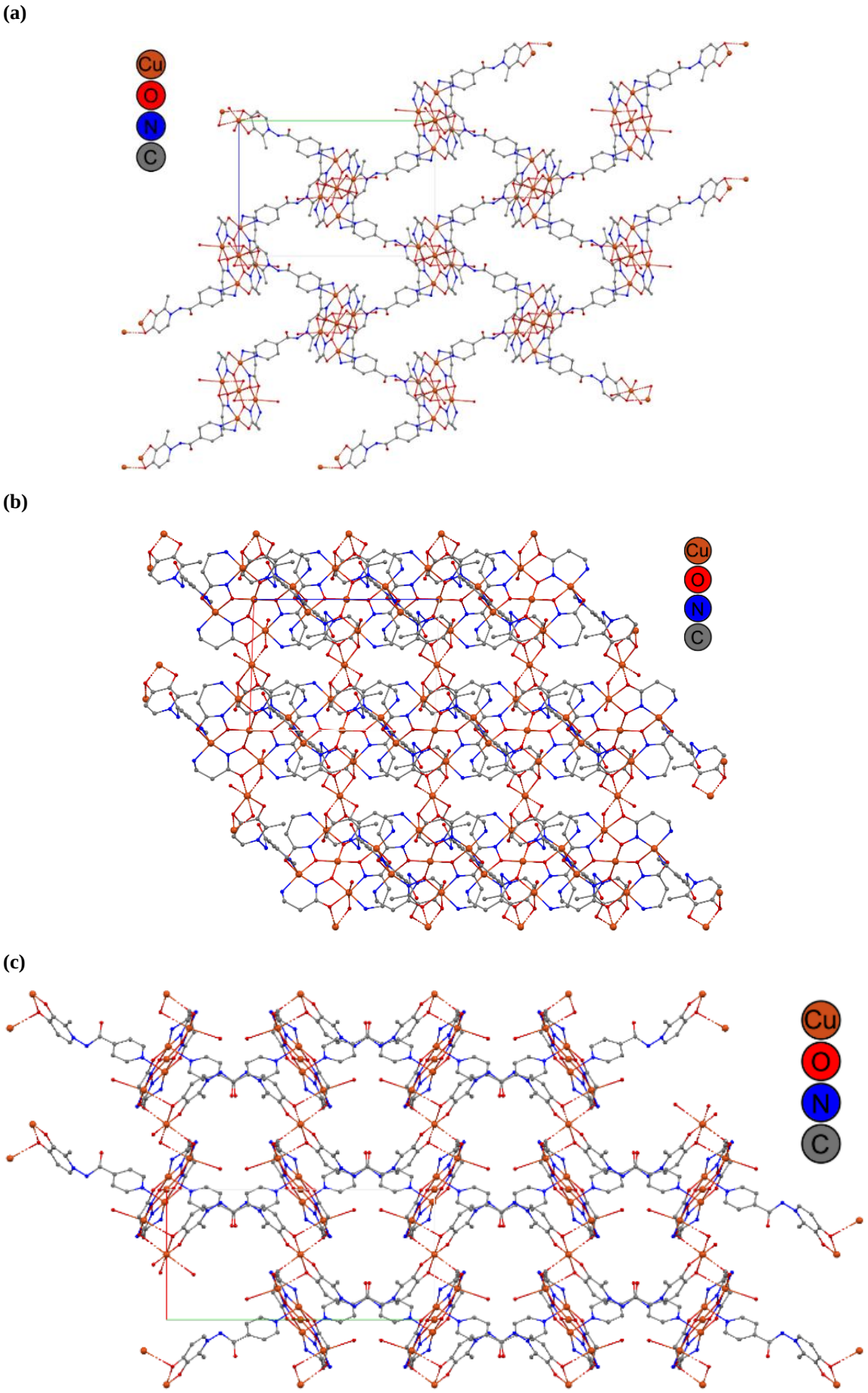

Figure S3. The 3D network of compound **1** along the (100), (010) and (001) vectors (figures **a**, **b** and **c**, respectively). "Guest" water molecules are omitted.

Table S1. The selected bond lengths [Å] and angles [°] in the compound **1**

Bond	**1**, Å	Angle	**1**, deg
Cu(1)-O(1)	1.870(2)	O(1)-Cu(1)-O(3)	90.57(9)
Cu(1)-O(3)	1.911(2)	O(1)-Cu(1)-O(3A)	89.43(9)
Cu(2)-O(1)	1.912(2)	O(1)-Cu(2)-O(2)	79.59(9)
Cu(2)-O(2)	1.998(2)	N(3A)-Cu(2)-N(4A)	93.71(12)
Cu(2)-N(3A)	1.980(3)	O(1)-Cu(2)-N(3A)	87.95(10)
Cu(2)-N(4A)	1.993(3)	O(2)-Cu(2)-N(4A)	97.55(11)
Cu(3)-O(3)	1.913(2)	O(3)-Cu(3)-O(4)	80.82(9)
Cu(3)-O(4)	1.976(2)	N(1)-Cu(3)-N(2)	93.91(11)
Cu(3)-N(1)	1.968(3)	O(3)-Cu(3)-N(1)	89.15(10)
Cu(3)-N(2)	1.968(3)	O(4)-Cu(3)-N(2)	95.94(11)
Cu(4)-O(5)	1.943(2)	O(5)-Cu(4)-O(6)	86.74(10)
Cu(4)-O(6)	1.917(2)	O(5)-Cu(4)-O(6A)	93.26(10)
Cu(2)-N(7)	2.325(3)	O(1)-Cu(2)-N(7)	104.17(11)
O(5)-C(7)	1.306(4)	O(2)-Cu(2)-N(7)	92.47(10)
O(6)-C(8)	1.329(4)	N(3A)-Cu(2)-N(7)	93.33(10)
C(7)-C(8)	1.431(5)	N(4A)-Cu(2)-N(7)	91.05(12)
O(7)-C(13)	1.276(4)	O(5)-C(7)-C(8)	117.7(3)
N(5)-N(6)	1.426(4)	O(6)-C(8)-C(7)	117.5(3)
N(6)-C(13)	1.314(4)	O(7)-C(13)-N(6)	127.3(3)

Table S2. The dihedral angles between flat fragments of L ligand in compound **1** and in the free 3-hydroxy-4-pyridinone-isonicotinamide molecule[S2].

$Plane_1/Plane_2$	Compound **1**, deg	3-hydroxy-4-pyridinone-isonicotinamide[S2], deg
Pyridinone/Pyridine	75.4	34.8
Pyridinone/NCO	78.8	65.4
Pyridine/NCO	26.0	30.6

Computational details

The DFT calculations were performed with the Gaussian09 software[S6] using the double-hybrid B2PLYP functional[S7] and correlation consistent cc-pVDZ basis set[S8]. Full geometry optimizations were carried out at the default convergence criteria. The neutral ligand LH_2 and cuprate $[CuL_2]^{2-}$ were treated as a closed-shell singlet and open-shell doublet, respectively. The Wiberg bond indices (WBI)[S9,S10] were calculated with the NBO 3.1 code incorporated in the Gaussian09. For comparison the WBI values were computed with the NBO 6.0 version[S11]. The maximum difference in the WBI's of the discussed covalent bonds obtained by the two codes was 0.003. Topological parameters of the electron density and atomic charges according to the quantum theory of atoms in molecules (QTAIM)[S12] were computed with the AIMAll software[S13]. The π-contributions into the localized orbital locator (π-LOL)[S14] and electron localization function (π-ELF)[S15] were generated for the optimized structures using the Multiwfn code[S16,S17]. An addition of an empirical D3 dispersion correction[S7(b)] to the B2PLYP functional did not lead to a noticeable variation of molecular parameters.

Table S3. Computed parameters of the $[CuL_2]^{2-}$ and LH_2 optimized structures.

Bond	*d*, Å	$\rho(\mathbf{r}_c)$, a.u.	ε	DI	WBI
$[CuL_2]^{2-}$					
Cu(4)–O(5)	1.961	0.082	0.009	0.456	0.321
Cu(4)–O(6)	1.945	0.086	0.015	0.477	0.345
C(7)–O(5)	1.301	0.332	0.001	0.995	1.244
C(8)–O(6)	1.317	0.322	0.017	0.968	1.155
C(8)–C(9)	1.405	0.302	0.317	1.149	1.402
C(10)–C(11)	1.389	0.306	0.290	1.246	1.478
C(7)–C(8)	1.447	0.289	0.190	0.980	1.154
C(7)–C(11)	1.412	0.298	0.228	1.130	1.301
N(5)–C(9)	1.379	0.297	0.217	0.962	1.139
N(5)–C(10)	1.352	0.316	0.205	1.014	1.241
N(5)–N(6)	1.419	0.310	0.034	1.012	0.988
C(13)–O(7)	1.250	0.374	0.040	1.068	1.500
N(6)–C(13)	1.345	0.341	0.207	1.062	1.391
LH_2					
C(7)–O(5)	1.249	0.374	0.024	1.132	1.541
C(8)–O(6)	1.350	0.295	0.003	0.892	1.023
C(8)–C(9)	1.370	0.320	0.396	1.270	1.571
C(10)–C(11)	1.368	0.317	0.322	1.345	1.640
C(7)–C(8)	1.466	0.279	0.149	0.924	1.081
C(7)–C(11)	1.442	0.285	0.154	1.019	1.155
N(5)–C(9)	1.400	0.285	0.173	0.898	1.039
N(5)–C(10)	1.371	0.303	0.118	0.951	1.127
N(5)–N(6)	1.383	0.339	0.026	1.038	1.009
C(13)–O(7)	1.217	0.402	0.068	1.154	1.714
N(6)–C(13)	1.394	0.299	0.098	0.851	1.070

Table S4. Effective atomic charges (in *e*) calculated using QTAIM.

Atom	$[CuL_2]^{2-}$	LH_2
O(5)	−1.146	−1.146
O(6)	−1.144	−1.155
C(7)	0.729	0.959
C(8)	0.680	0.535
C(9)	0.405	0.382
C(10)	0.490	0.451
C(11)	−0.030	−0.015
N(5)	−0.936	−0.872
N(6)	−0.772	−0.831
O(7)	−1.217	−1.152
C(13)	1.442	1.454
N(7)	−1.177	−1.138
Cu(4)	1.169	—
H(1)	—	0.639
H(2)	—	0.472

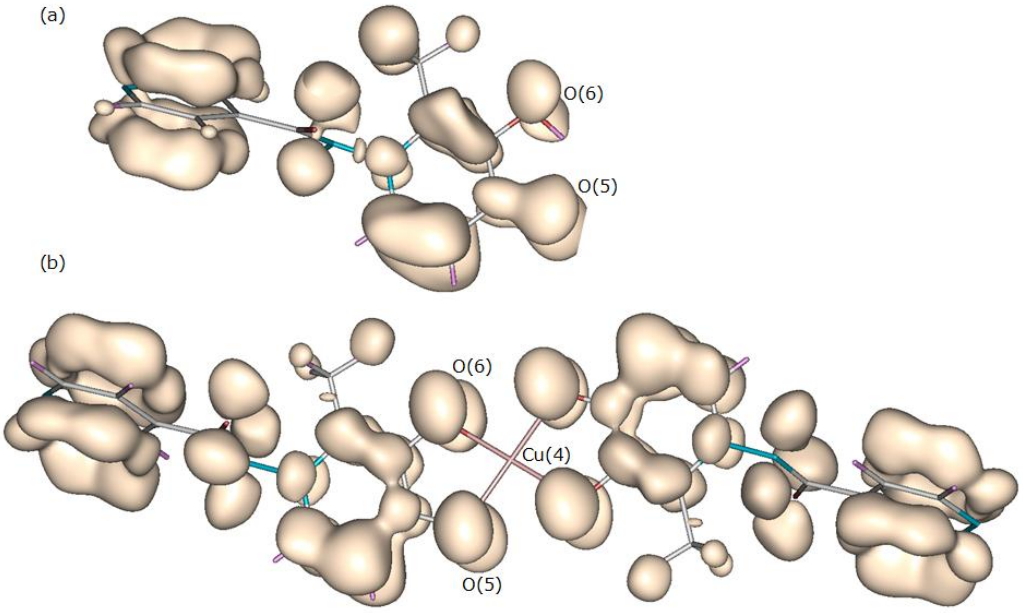

Figure S4. Distribution of the π-electron density in approximation by the π-ELF function (at value of 0.62) for LH_2 (a) and $[CuL_2]^{2-}$ (b).

Antimycobacterial activity

Paper Disk Assay

Biological activity of compounds was determined in *M. smegmatis* mc2 155 test systems by the Paper Disk Assay[S18]. A culture of *M. smegmatis* was grown as a lawn on an agar medium around paper disks with a diameter of 6 mm, soaked in solutions of the test compound in DMSO, having different concentrations. *M. smegmatis* grown on Tryptone soya agar M-290 (Himedia) were cultivated for a night in Lemco-TW liquid medium (Lab Lemco' Powder 5 g/L (Oxoid), Peptone special 5 g/L (Oxoid), NaCl 5 g/L, Tween-80) at 37 ◦C until logarithmic mean growth phase at optical density OD600 = 1.5. Bacteria were mixed with melt agar medium M-290 in ratio 1: 9: 10 (culture: Lemco-TW: M-290) and poured as the top layer onto Petri dishes with lower agar M-290. After the top layer had hardened, paper disks soaked in the test substances were placed on the surface. The culture was incubated for 24 h at 37 ◦C. The diameter of the growth inhibition zone (halo) of a *M. smegmatis* culture grown in a lawn on an agar medium around paper disks containing the test compound in different concentrations was quantified. The minimum inhibitory concentration (MIC) was considered to be the concentration of the compound at which the growth inhibition zone is minimal. As a technical control, the disk was impregnated with the solvent of each substance. Growth inhibition halos were measured with a digital caliper and analyzed in a Mega Bio-Print 3020-WL/LC/20M X-Press, Vilber Lourmat Gel Documentation System). The experiments were carried out as triplicate, and the average diameter and standard deviation (SD) were calculated. We used CLSI standards containing information about disk diffusion (M02) and dilution (M07, M11) test procedures for bacteria and Laboratory Practices in Microbiology[S19].

Table S5. Antibacterial activity of compounds against *M. smegmatis.*

Compound	MIC, nmole/disk	Diameter of growth inhibition zone, mm	
		24 h	72 h
$[Cu_5(\beta\text{-alaha}_4)](CuL_2)(H_2O)_{26}$ (**1**)	365	6.73±0.25*	6.5±0.1***
$Cu(ac)_2 \cdot H_2O$	2000	6.75±0.28*	6.4±0.18***
β-alaninehydroxamic acid	2000	6.4±0.1*	0**
3-hydroxy-4-pyridinone-isonicotinamide	4000	6.2±0.1*	6.1±0.05***
INH	730	6.45±0.2*	6.1±0.1***
RIF	6	6.9±0.15*	6.8±0.1*

* The inhibition zone diameter of *M. smegmatis* growth does not overgrow within the specified time.
** No growth inhibition zone.
*** The growth inhibition zone is overgrown at the edge.

References

S1 B. Kurzak, E. Farkas, T. Glowiak and H. Kozlowski, *J. Chem. Soc., Dalton Trans.*, 1991, 163; https://doi.org/10.1039/DT9910000163.

S2 M. A Katkova, G. S. Zabrodina, R. V. Rumyantcev, G. Yu. Zhigulin, I. V. Skabitsky, I. G. Fomina, O. B. Bekker, S. Yu. Ketkov and I. L. Eremenko, *Mendeleev Commun.*, 2024, **34**, 850; https://doi.org/10.1016/j.mencom.2024.10.026.

S3 Rigaku Oxford Diffraction, *CrysAlis Pro software system, version 1.171.42.76a*, Rigaku Corporation, Wroclaw, 2022.

S4 G. M. Sheldrick, *Acta Crystallogr*., *Sect. A: Found. Adv*., 2015, **71**, 3; https://doi.org/10.1107/S2053273314026370.

S5 G. M. Sheldrick, *Acta Crystallogr*., Sect. C: Struct. Chem., 2015, **71**, 3; https://doi.org/10.1107/S2053229614024218.

S6 M. J. Frisch, G. W. Trucks, H. B. Schlegel, G. E. Scuseria, M. A. Robb, J. R. Cheeseman, G. Scalmani, V. Barone, B. Mennucci, G. A. Petersson, H. Nakatsuji, M. Caricato, X. Li, H. P. Hratchian, A. F. Izmaylov, J. Bloino, G. Zheng, J. L. Sonnenberg, M. Hada, M. Ehara, K. Toyota, R. Fukuda, J. Hasegawa, M. Ishida, T. Nakajima, Y. Honda, O. Kitao, H. Nakai, T. Vreven, J. A. Montgomery, Jr., J. E. Peralta, F. Ogliaro, M. Bearpark, J. J. Heyd, E. Brothers, K. N. Kudin, V. N. Staroverov, T. Keith, R. Kobayashi, J. Normand, K. Raghavachari, A. Rendell, J. C. Burant, S. S. Iyengar, J. Tomasi, M. Cossi, N. Rega, J. M. Millam, M. Klene, J. E. Knox, J. B. Cross, V. Bakken, C. Adamo, J. Jaramillo, R. Gomperts, R. E. Stratmann, O. Yazyev, A. J. Austin, R. Cammi, C. Pomelli, J. W. Ochterski, R. L. Martin, K. Morokuma, V. G. Zakrzewski, G. A. Voth, P. Salvador, J. J. Dannenberg, S. Dapprich, A. D. Daniels, O. Farkas, J. B. Foresman, J. V. Ortiz, J. Cioslowski and D. J. Fox, *Gaussian 09, Revision E.01*, Gaussian Inc., Wallingford, CT, 2013.

S7 (*a*) S. Grimme, *J. Chem. Phys.*, 2006, **124**, 034108; https://doi.org/10.1063/1.2148954; (*b*) S. Grimme, J. Antony, S. Ehrlich and H. Krieg, *J. Chem. Phys*., 2010, **132,** 154104; https://doi.org/10.1063/1.3382344.

S8 T. H. Dunning, Jr., *J. Chem. Phys.*, 1989, **90**, 1007; https://doi.org/10.1063/1.456153.

S9 K. B. Wiberg, *Tetrahedron*, 1968, **24**, 1083; https://doi.org/10.1016/0040-4020(68)88057-3.

S10 E. D. Glendening and F. Weinhold, *J. Comp. Chem.*, 1998, **19**, 610; https://doi.org/10.1002/(SICI)1096-987X(19980430)19:6<610::AID-JCC4>3.0.CO;2-U.

S11 E. D. Glendening, C. R. Landis and F. Weinhold, *J. Comput. Chem.*, 2013, **34**, 1429; https://doi.org/10.1002/jcc.23266.

S12 R. F. W. Bader, *Atoms in Molecules: A Quantum Theory*, Oxford University Press, Oxford, UK, 1990.

S13 T. A. Keith, *AIMAll*, *Version 10.05.04*, TK Gristmill Software, Overland Park, KS, 2010.

S14 S. N. Steinmann, Y. Mo and C. Corminboeuf, *Phys. Chem. Chem. Phys.*, 2011, **13**, 20584; https://doi.org/10.1039/C1CP21055F.

S15 J. C. Santos, W. Tiznado, R. Contreras and P. Fuentealba, *J. Chem. Phys.*, 2004, **120**, 1670; https://doi.org/10.1063/1.1635799.

S16 T. Lu and F. Chen, *J. Comput. Chem.*, 2011, **33**, 580; https://doi.org/10.1002/jcc.22885.

S17 T. Lu and F. Chen, *J. Mol. Graph. Model.*, 2012, **38**, 314; https://doi.org/10.1016/j.jmgm.2012.07.004.

S18 S. G. Frolova, A. A. Vatlin, D. A. Maslov, B. Yusuf, G. I. Buravchenko, O. B. Bekker, K. M. Klimina, S. V. Smirnova, L. M. Shnakhova, I. K. Malyants, A. I. Lashkin, X. Tian, M. S. Alam, G. V. Zatonsky, T. Zhang, A. E. Shchekotikhin and V. N. Danilenko, *Pharmaceuticals*, 2023, **16,** 1565; https://doi.org/10.3390/ph16111565.

S19 O. Erkmen, in *Laboratory Practices in Microbiology*, Academic Press, Cambridge, MA, 2021, pp. 181–186.